LAWRENCE
LIVERMORE
NATIONAL
LABORATORY

UCRL-JRNL-213773

Young organic matter as a source of carbon dioxide outgassing from Amazonian rivers

E. Mayorga, A. K. Aufdenkampe, C. A. Masiello, A. V. Krusche, J. I. Hedges, P. D. Quay, J. E. Richey, T. A. Brown

July 20, 2005

Nature

Young organic matter as a source of carbon dioxide outgassing from Amazonian rivers

Emilio Mayorga[1], Anthony K. Aufdenkampe[2], Caroline A. Masiello[3], Alex V. Krusche[4], John I. Hedges[1,†], Paul D. Quay[1], Jeffrey E. Richey[1] & Thomas A. Brown[5]

[1]*School of Oceanography, University of Washington, Seattle, WA 98195, USA*

[2]*Stroud Water Research Center, Avondale, PA 19311, USA*

[3]*Department of Earth Science, Rice University, Houston, TX 77005, USA*

[4]*Laboratório de Ecologia Isotópica, CENA-USP, 13400-970 Piracicaba SP, Brazil*

[5]*Center for Accelerator Mass Spectrometry, Lawrence Livermore National Laboratory, Livermore, CA 94551, USA*

E.M. and A.K.A. contributed equally to this work.

Correspondence and request for materials should be addressed to E.M. (emiliomayorga@alum.mit.edu).

[†]Deceased.

Rivers are generally supersaturated with respect to carbon dioxide, resulting in large gas evasion fluxes that can be a significant component of regional net carbon budgets[1,2]. Amazonian rivers were recently shown to outgas more than ten times the amount of carbon exported to the ocean in the form of total organic carbon or dissolved inorganic carbon[1]. High carbon dioxide concentrations in rivers originate largely from *in situ* respiration of organic carbon[1-3], but little agreement exists about the sources or turnover times of this carbon[2,4,5]. Here we present results of an extensive survey of the carbon isotope composition (^{13}C and ^{14}C) of dissolved inorganic carbon and three size-fractions of organic carbon across the Amazonian river system. We find that respiration of contemporary organic

matter (less than 5 years old) originating on land and near rivers is the dominant source of excess carbon dioxide that drives outgassing in mid-size to large rivers, although we find that bulk organic carbon fractions transported by these rivers range from tens to thousands of years in age. We therefore suggest that a small, rapidly cycling pool of organic carbon is responsible for the large carbon fluxes from land to water to atmosphere in the humid tropics.

Riverine CO_2 concentrations in Amazonian lowlands are 5-30 times supersaturated with respect to atmospheric equilibrium[1]; such conditions may be prevalent throughout the humid tropics. *In situ* respiration is the primary source of CO_2 sustaining supersaturation in rivers, although inputs from groundwater supersaturated by soil respiration can be important in small systems and from submerged riparian root respiration in floodplain influenced systems[1-3,6-8]. While air-water gas exchange is a bi-directional process, atmospheric CO_2 invasion has a negligible role compared to the large CO_2 evasion fluxes, except at low supersaturation[2,3,6,7]. ^{13}C and ^{14}C isotopes can provide constraints on sources and turnover times of organic carbon (OC) fuelling river respiration, yet no previous tropical study has used a dual-isotope approach to address these questions. Studies in temperate eastern USA provide contrasting findings. In the Hudson River, up to 70% of the centuries-old terrestrial OC entering the river is respired in transit, and the average age of riverine OC decreases downstream[2]. However, the youngest components of dissolved OC (DOC) are preferentially respired in the York River[5], and modern dissolved inorganic carbon (DIC) in the Parker River may be explained by respiration of young DOC produced within the estuary[4]. Documenting key patterns and controls on CO_2 sources in diverse ecosystems is critical to advance our understanding of CO_2 outgassing from rivers and its contribution to regional net carbon budgets.

To identify dominant sources and turnover times of riverine carbon throughout the Amazon basin, we analysed ^{14}C and ^{13}C of DIC, DOC, and suspended fine and coarse particulate OC fractions (FPOC and CPOC), grouping sites topographically (Fig. 1). This survey represents the most extensive dual carbon isotope inventory to date in a large, diverse basin, and the first ^{14}C analysis of DIC in Amazonian rivers. It complements but greatly exceeds previous carbon isotope surveys[5,7,9], enabling an integrated assessment of carbon cycling.

DIC is composed of dissolved CO_2 and bicarbonate and carbonate ions in pH-dependent chemical and isotopic equilibrium[10]. In studies of marine and homogeneous river systems, where pH is nearly uniform, it has been the convention to report the isotopic composition of total DIC, which is directly measured. However, when the turnover of DIC by CO_2 fluxes is as rapid as in many of these tropical rivers, a quasi-steady-state condition constrains the isotopic composition of outputs by CO_2 outgassing to equal that of inputs by CO_2 production from respiration[7,8]. In response to this pre-eminence of CO_2 sources and the large range of observed pH (3.8 to 8.7), we base our analysis on the calculated isotopic values of CO_2 gas in equilibrium with DIC, avoiding the need to discuss the isotopic variation in ^{13}C of DIC caused by changes in pH alone (see Methods and Supplementary Discussion). We report measured $\delta^{13}C$-DIC in Table S3. For ^{14}C we use $\Delta^{14}C$ notation, which includes a correction for ^{13}C such that $\Delta^{14}C$ of CO_2 and DIC are equal at any pH (ref. 11).

CO_2 in nearly all lowland rivers had a $\Delta^{14}C$ signature bound within the range of local atmospheric $\Delta^{14}C$-CO_2 estimated for the lowland DIC sampling period (1996-2003, Fig. 2; Methods). Testing of thermonuclear bombs resulted in a large increase in atmospheric $^{14}CO_2$, reaching a peak in the late 1960s and steadily decreasing afterwards[12,13]. Continual change in atmospheric radiocarbon content necessitates that we assess the mean age for modern carbon samples by the offset between riverine $\Delta^{14}C$

and the sampling year's annual mean atmospheric $\Delta^{14}C\text{-}CO_2$ (ref. 14). From 1996 to 2003, $\Delta^{14}C\text{-}CO_2$ at four supersaturated sites in mid to large lowland rivers decreased by 32-42‰, equivalent to the annually averaged atmospheric $\Delta^{14}C\text{-}CO_2$ decrease of 36‰ (-5.6±2.3‰ yr^{-1}) (Fig. 3). Thus, atmospheric offsets remained roughly constant, suggesting constant respiratory OC turnover times for each basin. The range of these offsets suggests rapid turnover of photosynthetically sequestered atmospheric CO_2; outgassed CO_2 is derived from atmospheric CO_2 sequestered within <4 years in the mid-sized Ji-Parana basin ($\Delta^{14}C$ offsets: 14±6‰, n=8) and 4-7 years previously at the Rio Negro mouth ($\Delta^{14}C$ offsets: 29±9‰, n=3).

Rapid carbon turnover is likely widespread across Amazonian rivers. However, DIC from carbonate mineral weathering, with its typically enriched $\delta^{13}C$ and highly depleted $\Delta^{14}C$ (Fig. 2), commonly obscures the influence of respiration. To focus on sites where DIC originates largely as respired CO_2, we identified sites draining substantial carbonate lithologies through their inorganic solute composition[15] (Methods and Supplementary Discussion). Only lowland sites had little potential for direct, substantial carbonate contributions to DIC (38 samples in 25 lowland sites, Fig. S1). Observations in carbonate-free lowlands contained supersaturated, predominantly contemporary CO_2 (Table 1, Fig. 2) and could be divided into two groups based on atmospheric $\Delta^{14}C\text{-}CO_2$ offsets. The largest group (32 samples from 21 sites) encompassed first-order streams and large rivers carrying contemporary CO_2 with atmospheric $\Delta^{14}C\text{-}CO_2$ offsets ranging from -3 to 38‰ (14±11‰), indicating a mean CO_2 age of approximately 2 years, and <5 years in 87% of the observations; enriched $\delta^{13}C\text{-}CO_2$ in the Ji-Parana region (-17.5±2.2‰, n=21) suggest a C_4 plant influence. The second group of carbonate-free observations consisted of 6 samples in 3 small and 2 mid-sized rivers in the Ji-Parana region having considerable negative $\Delta^{14}C$ offsets (-32±21‰), indicating a mean source age of several decades. Relatively depleted $\delta^{13}C\text{-}CO_2$ values (-20.0±1.7‰) compared to Ji-Parana rivers from the first group suggest an

influence from groundwater influx of aged soil CO_2 with a significant terrestrial C_3 plant source relative to other rivers in that highly deforested region. In both groups, respiration of submerged tree and grass roots can be excluded as important CO_2 sources because our dataset was predominantly collected during low water.

Isotopic signatures in carbonate-free lowland rivers demonstrate that CO_2 originated from heterotrophic respiration of contemporary C_3 and C_4 organic carbon (Fig. 2), yet CO_2 appears isotopically distinct from the associated bulk OC load. All OC fractions were considerably depleted in ^{13}C relative to CO_2 (Table 1, Fig. 2, and Supplementary Discussion). Furthermore, DOC was generally older than CO_2, FPOC showed a bimodal distribution with ages similar to CO_2 in non-turbid rivers and older carbon in high-sediment rivers, and CPOC exhibited a wide range of ages. We conclude that *in situ* respiration is fuelled largely by an unmeasured organic subfraction that cycles on the order of <5 years and typically makes up a small component of the riverine OC load. ^{13}C enrichment of CO_2 relative to OC indicates that this missing OC source fuelling river respiration is disproportionately composed of riparian and floodplain C_4 grasses, which may be intrinsically more biodegradable[7,16].

Mountain and mixed rivers contain older dissolved CO_2 ($\Delta^{14}C$ = –749 to 96‰) with clear carbonate mineral dissolution signatures. However, observed CO_2 supersaturation in these rivers must be generated by CO_2 sources other than carbonates (Supplementary Discussion). These CO_2 fluxes gradually flush out geologically derived DIC, replacing its isotopic signature. Indeed, a CO_2 trend of increasing $\Delta^{14}C$ and decreasing $\delta^{13}C$ is observed from the Peruvian Andes to the Amazon mainstem, with $\Delta^{14}C$-CO_2 reaching 30-76‰ in the central mainstem, still below atmospheric levels (Fig. 2). Along the Ucayali and western-central mainstem, inputs of likely young CO_2 from *in situ* respiration and lowland tributaries drive large evasion fluxes of ^{14}C-depleted CO_2 derived from carbonate dissolution. In the more arid Ucayali mountain

headwaters, highly depleted $\Delta^{14}C\text{-}CO_2$ (<-500‰), enriched $\delta^{13}C\text{-}CO_2$ (~ -11‰), and considerable CO_2 supersaturation point to solid-earth degassing as a large dry-season CO_2 source, as documented in other tectonically active mountain ranges[17].

Control of respiration by a small fraction of OC does not imply that bulk OC is unreactive. On the contrary, measured OC fractions appear to be mineralised throughout the river system. The strongest evidence is that FPOC generally becomes younger and more depleted in ^{13}C downstream from mountain sites (Fig. 2, Table 1), where all OC fractions mirror the high-altitude ^{13}C enrichment in plants of ~ 1‰ per 1000 m elevation[18,19]. Within 1000 km from mountain headwaters, $\delta^{13}C$-FPOC becomes nearly undistinguishable from lowland carbon. With FPOC tightly associated with mineral surfaces[19,20], no downstream changes in the ratio of FPOC to fine suspended sediment concentration (0.8-1.5%, Table S2), and >85% of the Amazon mainstem mineral load ultimately originating in the Andes[21], this observation implies nearly complete mineralization of old Andean FPOC and replacement with new lowland OC during transit within the river or during long-term flooplain storage[7]. Even if all FPOC leaving the Andes were mineralised within the river channel, the resulting CO_2 flux would be 1/40 of total CO_2 evasion fluxes[1], hardly impacting the isotopic signature of CO_2. CPOC and DOC descending from the Andes follow identical trends of gradual ^{13}C depletion to lowland values (Fig. 2), although without a conservative mineral carrier as for FPOC, simple dilution by lowland OC can not be ruled out. DOC is generally modern (<50 years old) everywhere, demonstrating that old DOC does not escape from the basin.

Isotopic evidence for dominance of respiration fluxes by a rapidly cycling, typically small fraction of total OC confirms the hypothesis previously posited for the Amazon mainstem from respiration[8,16], ^{13}C (ref. 7), and mass balance studies[1,7]. It implies that gradual consumption or replacement of old fractions in bulk OC can occur in parallel

with high rates of respiration of a highly labile OC subfraction. This paradigm has been advanced for tropical and temperate soils[22], providing strong conceptual linkage between aquatic and terrestrial carbon dynamics[23]. It suggests that deforestation in Amazonia leads to immediate changes to the organic sources of riverine heterotrophic energy and argues that such impact is not inconsistent with apparent lag times observed in bulk OC composition[24]. While the mechanism proposed here may be widespread across the humid tropics[1] and appears consistent with radiocarbon observations from temperate rivers[2,4,5], it is probable that certain river systems, such as those draining eroding peats, are fuelled by old organic carbon. Explicit accounting of isotopic signatures of CO_2 outgassing from different river types may be required to accurately interpret isotope-based regional tropospheric CO_2 inversions.

Methods

Sample collection and analysis. Samples analysed for ^{14}C-DIC were collected between 1991 and 2003, whereas ^{14}C-OC samples are from 1995-1996. All samples were preserved with mercuric chloride immediately after collection at mid-depth from the deepest section of the channel. DIC samples were prepared as described in Quay *et al.*[7] and stored in tightly capped glass bottles for up to 24 months; in the lab, the top half of the bottle was drawn into a vacuum line (eliminating particles) and stripped of CO_2 after acidification[7]. CPOC (63-2000 μm) was isolated either by sieving or with a plankton net, FPOC (0.1-63 μm) by tangential flow microfiltration, and DOC (1000 atomic mass units to 0.1 μm) by tangential flow ultrafiltration[19]; final concentration and drying was achieved by centrifugal evaporation or freeze drying[19], and the dried powder stored in the dark at ambient temperature for up to 6 years. Ultrafiltration yields ranged from 40% in the Andes to 80% in the lowlands[19,25]. Organic samples were combusted as in Quay *et al.*[7]. Cryogenically purified CO_2 from OC and DIC was analysed for stable isotope and radiocarbon by dual-inlet Isotope Ratio Mass Spectrometry and

Accelerator Mass Spectrometry (AMS)[26], respectively; > 90% of ^{14}C analyses were carried out at the Lawrence Livermore National Laboratory's Center for Accelerator Mass Spectrometry, and the rest at the University of Arizona AMS Laboratory. CO_2 extracted from DIC was stored in sealed glass ampules for up to 8 years. ^{13}C is reported in $\delta^{13}C$ notation vs. the PDB standard[10]. Radiocarbon values are reported as age-corrected $\Delta^{14}C$ adjusted for sample $\delta^{13}C$ (ref. 11); carbon is defined as modern when it originates after 1890 (ref. 11). Absolute $\Delta^{14}C$ and $\delta^{13}C$ analysis errors (1σ) are typically <6‰ and <0.2‰, respectively. Isotopes for all carbon fractions were not always analysed at each site. Additional analyses include pH, major ions, alkalinity, and total carbon fraction concentrations (Table S2). Major ions were quantified by ion chromatography. Alkalinity was measured by Gran titration, or estimated from temperature, pH, and DIC when not measured. CO_2 concentrations were either measured directly by headspace equilibration (Aufdenkampe, manuscript in preparation) or estimated from temperature, pressure, pH, DIC, and alkalinity. Sampling sites are grouped by topographic characteristics (Fig. 1). In the discussion, grouped observations are reported as mean ± standard deviation (number of samples) and compared only qualitatively due to low number of samples per group.

Isotopic calculation of CO_2 gas in equilibrium with DIC. DIC is composed of dissolved carbonate species (H_2CO_3(aq), HCO_3^-(aq), and CO_3^{2-}(aq)) in pH- and temperature-dependent equilibrium with one another. Isotopic fractionation occurs during conversion from one species to another and dissolution of CO_2 gas[10]; CO_2 gas is hereafter referred to as simply CO_2. $\delta^{13}C$ of CO_2 gas in equilibrium with DIC is calculated from measured $\delta^{13}C$-DIC and pH, and from temperature-dependent isotopic equilibrium fractionations between CO_2 and DIC species[10,27]. pH can vary dramatically in a large basin and is largely a function of weathering lithologies (Table S2). $\Delta^{14}C$ is defined to be insensitive to mass-dependent fractionation[11]; as a result $\Delta^{14}C$-CO_2 = $\Delta^{14}C$-DIC. While a focus on isotopes of CO_2 instead of DIC is unconventional, it yields

more straightforward assessments of the impact of respiration and air-water gas exchange on DIC across geochemically diverse rivers.

Radiocarbon trends in atmospheric CO_2. Measurements from Schauinsland Station, Germany, were used to characterise atmospheric $\Delta^{14}C$-CO_2 from 1991 to 2003 (refs. 12,14). The uncharacterised effect of seasonal and short-term atmospheric variability is minimized by comparing river ^{14}C only against time-weighted annual means[14]. A constant +8‰ offset was added to Schauinsland annual means to account for a 5‰ depletion from regional fossil-fuel emissions at Schauinsland relative to the well-mixed, mid-latitude European troposphere (Jungfraujoch site[14]), and approximately 3‰ further depletion at the mid-latitude troposphere relative to tropical South America[12,13]. Atmospheric $\Delta^{14}C$-CO_2 composition within the Amazon basin is unknown, but seasonal and regional variability may be as large as 10‰ (ref. 13). Riverine $\Delta^{14}C$ values within 5‰ of our estimated atmospheric annual average for the sampling year likely represent carbon turnover times of one year or less. Mid-1990s tropospheric CO_2 can be characterized by a partial pressure (pCO_2) of 370 ppm and $\delta^{13}C$ composition of -8‰ (refs. 10,12,13).

Carbonate mineral dissolution and DIC. Carbonate weathering is a source of high DIC concentrations enriched in $\delta^{13}C$ and highly depleted in $\Delta^{14}C$ when, as is most common, it involves the dissolution of ^{14}C-dead carbonate minerals ($CaCO_3(s)$) by carbonic acid ($H_2CO_3(aq)$) from respired modern plant matter in soils (Fig. 2 and Supplementary Discussion). We used alkalinity and dissolved inorganic cation composition to identify sites draining substantial carbonate lithologies[15] (Fig. S1). While exchange with the atmosphere or input of respired CO_2 may erase the isotopic signature of carbonate dissolution, we identified and excluded carbonate-influenced sites in order to unambiguously focus on the isotopic relationship between organic carbon and DIC.

1. Richey, J. E., Melack, J. M., Aufdenkampe, A. K., Ballester, M. V. & Hess, L. L. Outgassing from Amazonian rivers and wetlands as a large tropical source of atmospheric CO_2. *Nature* **416**, 617-620 (2002).

2. Cole, J. J. & Caraco, N. F. Carbon in catchments: Connecting terrestrial carbon losses with aquatic metabolism. *Marine and Freshwater Research* **52**, 101-110 (2001).

3. Mulholland, P. J. *et al.* Inter-biome comparison of factors controlling stream metabolism. *Freshwater Biology* **46**, 1503-1517 (2001).

4. Raymond, P. A. & Hopkinson, C. S. Ecosystem modulation of dissolved carbon age in a temperate marsh-dominated estuary. *Ecosystems* **6**, 694-705 (2003).

5. Raymond, P. A. & Bauer, J. E. Riverine export of aged terrestrial organic matter to the North Atlantic Ocean. *Nature* **409**, 497-500 (2001).

6. Jones, J. B. & Mulholland, P. J. Carbon dioxide variation in a hardwood forest stream: An integrative measure of whole catchment soil respiration. *Ecosystems* **1**, 183-196 (1998).

7. Quay, P. D. *et al.* Carbon cycling in the Amazon River: Implications from the ^{13}C compositions of particles and solutes. *Limnology and Oceanography* **37**, 857-871 (1992).

8. Devol, A. H. & Hedges, J. I. in *The Biogeochemistry of the Amazon Basin* (eds. McClain, M. E., Victoria, R. L. & Richey, J. E.) 275-306 (Oxford University Press, New York, 2001).

9. Hedges, J. I. *et al.* Organic carbon-14 in the Amazon River system. *Science* **231**, 1129-1131 (1986).

10. Clark, I. & Fritz, P. *Environmental Isotopes in Hydrogeology* (Lewis Publishers, Boca Raton, 1997).

11. Stuiver, M. & Polach, H. A. Discussion: Reporting of ^{14}C data. *Radiocarbon* **19**, 355-363 (1977).

12. Levin, I. & Hesshaimer, V. Radiocarbon -- A unique tracer of global carbon cycle dynamics. *Radiocarbon* **42**, 69-80 (2000).

13. Randerson, J. T., Enting, I. G., Schuur, E. A. G., Caldeira, K. & Fung, I. Y. Seasonal and latitudinal variability of troposphere $\Delta^{14}CO_2$: Post bomb contributions from fossil fuels, oceans, the stratosphere, and the terrestrial biosphere. *Global Biogeochemical Cycles* **16**, 1112, doi:10.1029/2002GB001876 (2002).

14. Levin, I. & Kromer, B. The tropospheric $^{14}CO_2$ level in mid-latitudes of the Northern Hemisphere (1959-2003). *Radiocarbon* **46**, 1261-1272 (2004).

15. Stallard, R. F. & Edmond, J. M. Geochemistry of the Amazon. 2. The influence of geology and weathering environment on the dissolved load. *Journal of Geophysical Research* **88**, 9671-9688 (1983).

16. Melack, J. M. & Forsberg, B. R. in *The Biogeochemistry of the Amazon Basin* (eds. McClain, M. E., Victoria, R. L. & Richey, J. E.) 235-274 (Oxford University Press, New York, 2001).

17. Kerrick, D. M. Present and past nonanthropogenic CO_2 degassing from the solid earth. *Reviews of Geophysics* **39**, 565-585 (2001).

18. Körner, C., Farquhar, G. D. & Wong, S. C. Carbon isotope discrimination by plants follows latitudinal and altitudinal trends. *Oecologia* **88**, 30-40 (1991).

19. Hedges, J. I. *et al.* Organic matter in Bolivian tributaries of the Amazon River: A comparison to the lower mainstem. *Limnology and Oceanography* **45**, 1449-1466 (2000).

20. Aufdenkampe, A. K., Hedges, J. I., Richey, J. E., Krusche, A. V. & Llerena, C. A. Sorptive fractionation of dissolved organic nitrogen and amino acids onto fine

sediments within the Amazon Basin. *Limnology and Oceanography* **46**, 1921-1935 (2001).

21. Gibbs, R. J. The geochemistry of the Amazon River system: Part I. The factors that control the salinity and the composition and concentration of the suspended solids. *Geological Society of America Bulletin* **78**, 1203-1232 (1967).

22. Trumbore, S. E. Age of soil organic matter and soil respiration: Radiocarbon constraints on belowground C dynamics. *Ecological Applications* **10**, 399-411 (2000).

23. Grimm, N. B. *et al.* Merging aquatic and terrestrial perspectives of nutrient biogeochemistry. *Oecologia* **442**, 485–501 (2003).

24. Bernardes, M. C. *et al.* Riverine organic matter composition as a function of land use changes, Southwest Amazon. *Ecological Applications* **14**, S263-S279 (2004).

25. Aufdenkampe, A. K. *et al.* Organic matter in the Peruvian headwaters of the Amazon: A comparison to Bolivian tributaries and the lowland Amazon mainstem. *Organic Geochemistry* (in press).

26. Vogel, J. S., Nelson, D. E. & Southon, J. R. ^{14}C background levels in an accelerator mass spectrometry system. *Radiocarbon* **29**, 323-333 (1987).

27. Zhang, J., Quay, P. D. & Wilbur, D. O. Carbon isotope fractionation during gas-water exchange and dissolution of CO_2. *Geochimica et Cosmochimica Acta* **59**, 107-114 (1995).

28. Gesch, D. B., Verdin, K. L. & Greenlee, S. K. New land surface digital elevation model covers the Earth. *EOS* **80**, 70-71 (1999).

29. Mayorga, E., Logsdon, M. G., Ballester, M. V. R. & Richey, J. E. Estimating cell-to-cell land surface flow paths from digital channel networks, with an application to the Amazon basin. *Journal of Hydrology* (in press).

30. Hedges, J. I. *et al.* Compositions and fluxes of particulate organic material in the Amazon River. *Limnology and Oceanography* **31**, 717-738 (1986).

Acknowledgments. We thank staff at the Lawrence Livermore National Laboratory Center for Accelerator Mass Spectrometry (LLNL CAMS) for assistance with radiocarbon analyses; C. Llerena (Peru), B. Forsberg (Brazil), L. Maurice-Bourgoin (France-IRD), and J. Quintanilla (Bolivia) for invaluable assistance with field campaigns; and I. Levin (Heidelberg) for assistance with atmospheric $^{14}CO_2$ data. This work was funded by a LLNL CAMS Minigrant, US NSF DEB, NASA EOS and LBA projects, the Brazilian FAPESP agency, and a NASA ESS graduate fellowship to E.M. This work was performed, in part, under the auspices of the U.S. Department of Energy by University of California, Lawrence Livermore National Laboratory under contract W-7405-Eng-48. We dedicate this paper to the memory of J.I. Hedges.

Supplementary Information accompanies the paper on www.nature.com/nature.

Competing interests statement. The authors declare that they have no competing financial interests.

Table 1. Summary of ^{14}C and ^{13}C isotopic composition for each carbon fraction, by topographical site category. All carbonate-free sites are in the lowlands.

Site	CO_2		DOC		FPOC		CPOC	
Category	$\Delta^{14}C$	$\delta^{13}C$	$\Delta^{14}C$	$\delta^{13}C$	$\Delta^{14}C$	$\delta^{13}C$	$\Delta^{14}C$	$\delta^{13}C$
Mountain	-240±233 (14)	-12.9±2.2	94±176 (6)	-26.0±3.0	-202±198 (8)	-25.7±1.7	-39±146 (9)	-27.0±1.6
Mixed	-14±99 (11)	-19.4±1.2	196±59 (9)	-29.0±0.6	-135±141 (10)	-28.2±0.9	-124±66 (9)	-27.7±0.9
Lowland	89±44 (43)	-20.1±3.6	177±64 (15)	-29.0±0.9	90±55 (10)	-29.8±1.8	112±83 (4)	-28.5±0.7
Carbonate-free	98±20 (38)	-19.8±3.7	175±67 (11)	-29.1±0.7	129±10 (6)	-29.2±2.1	121±100 (3)	-28.4±0.9

Data are reported as mean ± standard deviation (number of samples), in per mil (‰). The number of samples for ^{13}C is the same as that shown for ^{14}C. $\delta^{13}C$-DIC summary values are -4.9±2.7‰ (mountain), -14.2±2.9‰ (mixed), -17.0±5.9‰ (lowland), and -17.1±6.2‰ (carbonate-free).

Figure 1. Amazon basin and river sites sampled for carbon isotopes. We used GTOPO30 elevation[28] and a regional river network dataset[29] to categorize each site by topography according to the percent of the drainage area above 1000 meter elevation: mountain (diamond), ≥ 50% (16 sites); mixed (square), ≥ 10% (11 sites); and lowland (circle), < 10% (33 sites). Mountain sites are found only in the Andean Cordillera, while mixed sites are large rivers draining both mountain and lowland areas. Site numbers are displayed. Distribution of sites by drainage area (river size) and mean basin elevation is inset. Additional information is in Supplementary Table S1.

Figure 2. Distribution of ^{14}C and ^{13}C isotopes. Lower $\Delta^{14}C$ values indicate older carbon. Symbol shapes as in as in Fig. 1; Red (shaded), blue, orange, and

green symbols represent CO_2, DOC, FPOC, and CPOC respectively. Isotopic ranges of carbon sources are shown by grey boxes. Plant $\delta^{13}C$ ranges from -32‰ to -26‰ for lowland plant material fixed via the C_3 photosynthetic pathway dominant among plants, to -16‰ to -12‰ for tropical C_4 grasses[24,30]. Phytoplankton take up H_2CO_3 and impose ^{13}C fractionations of ~-20‰, leading to biomass $\delta^{13}C$ values of -32 to -45‰ in mixed and lowland rivers[8,10,30], beyond the range found in our lowland OC and CO_2 observations. Carbonate rocks and CO_2 from solid earth degassing are ^{14}C-free ($\Delta^{14}C$ = -1000‰) (ref. 10). $\delta^{13}C$ of carbonate rocks is ~0‰; degassed CO_2 ranges from -6‰ for volcanic to 10‰ for metamorphic sources[10]. The carbonate weathering region represents CO_2 in equilibrium with HCO_3^- resulting from weathering by CO_2 derived from respired, contemporary C_3 or C_4 plant material[10].

Figure 3. Temporal evolution of ^{14}C-CO_2 at four lowland sites from mid-to-large rivers in the Ji-Parana basin and Rio Negro. Legend is as in Fig. 1. These sites drain continental shields and were analysed for ^{14}C-DIC 2–3 times between 1996 and 2003.

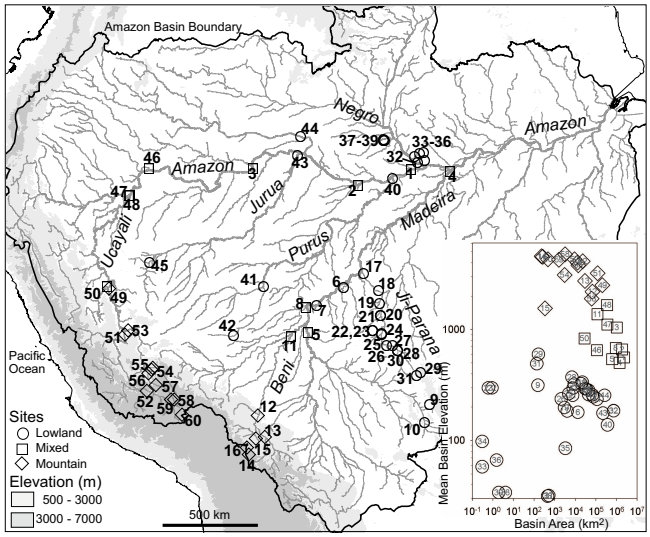
Amazon Basin Boundary
Negro
Amazon
Amazon
Jurua
Madeira
Purus
Ucayali
Ji-Parana
Beni
Pacific Ocean
Sites
Lowland
Mixed
Mountain
Elevation (m)
500 - 3000
3000 - 7000
500 km
Mean Basin Elevation (m)
Basin Area (km²)

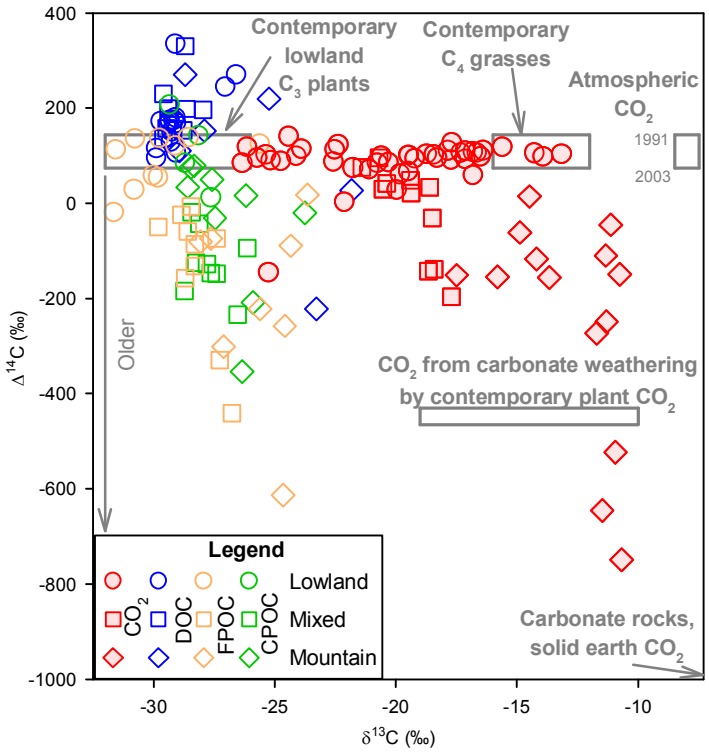
Contemporary lowland C3 plants
Contemporary C4 grasses
Atmospheric CO2
1991
2003
Older
CO2 from carbonate weathering by contemporary plant CO2
Carbonate rocks, solid earth CO2
Legend
CO2
DOC
FPOC
CPOC
Lowland
Mixed
Mountain
Δ14C (‰)
δ13C (‰)
400
200
0
-200
-400
-600
-800
-1000
-30
-25
-20
-15
-10

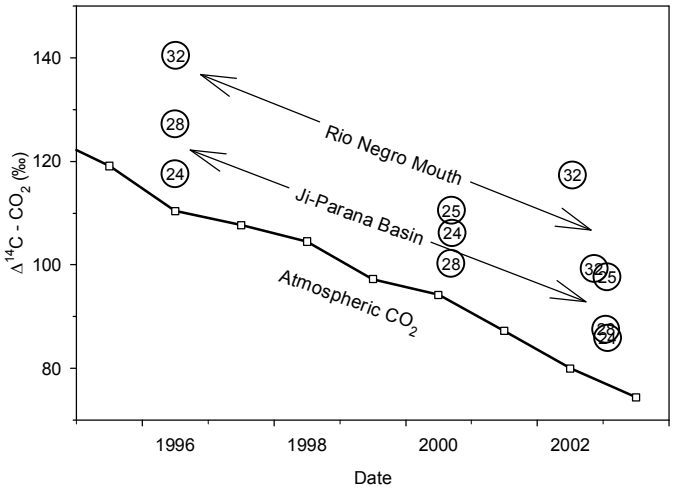
140
120
100
80
1996
1998
2000
2002
Date
Δ14C - CO2 (‰)
Rio Negro Mouth
Ji-Parana Basin
Atmospheric CO2
32
28
24
32
25
24
28
32
25

Young organic matter as a source of carbon dioxide outgassing from Amazonian rivers

Emilio Mayorga[1], Anthony K. Aufdenkampe[2], Caroline A. Masiello[3], Alex V. Krusche[4], John I. Hedges[1,†], Paul D. Quay[1], Jeffrey E. Richey[1] & Thomas A. Brown[5]

[1]*School of Oceanography, University of Washington, Seattle, WA 98195, USA*

[2]*Stroud Water Research Center, Avondale, PA 19311, USA*

[3]*Department of Earth Science, Rice University, Houston, TX 77005, USA*

[4]*Laboratório de Ecologia Isotópica, CENA-USP, 13400-970 Piracicaba SP, Brazil*

[5]*Center for Accelerator Mass Spectrometry, Lawrence Livermore National Laboratory, Livermore, CA 94551, USA*

E.M. and A.K.A. contributed equally to this work.

Correspondence and request for materials should be addressed to E.M. (emiliomayorga@alum.mit.edu).

[†]Deceased.

Supplementary Discussion

Use of calculated $\delta^{13}C$ of CO_2 gas versus measured $\delta^{13}C$ of DIC. There are two approaches to using stable isotopes to constrain sources contributing to pool – the mass balance approach, which requires an accounting of all fluxes and all species in a pool, and the steady-state approach, which only requires an accounting of the fluxes in and out of a pool. We use the latter approach in this paper, for reasons that can be illustrated by a thought experiment. Imagine two bottles of water at 25°C, each being sparged with bubbles of CO_2 with a $\delta^{13}C$ = -27.0‰. Bottle #1 is buffered to have a final pH of 3.8 at equilibrium, and the other a final pH of 8.7. These represent the extremes

of pH values observed in our Amazon data set (Table S2). Dissolved CO_2 will speciate into bicarbonate (HCO_3^-) and carbonate (CO_3^{2-}) ions as a function of pH, with the following enrichment factors (ε) for these reactions[10,27]:

$CO_2(g) + H_2O \leftrightarrow H_2CO_3$ ε = -1.2‰

$H_2CO_3 \leftrightarrow H^+ + HCO_3^-$ ε = +9.1‰

$HCO_3^- \leftrightarrow H^+ + CO_3^{2-}$ ε = -2.0‰

Partitioning of DIC into each species is calculated using standard, temperature-dependent equilibrium constants[10]. In bottle #1, 99.7% of the DIC will be in the form of H_2CO_3, whereas in bottle #2, 97.3% of the DIC is found as HCO_3^-. At steady state the $\delta^{13}C$ of DIC in these two bottles will be -28.2‰ and -19.2‰, respectively. pH has a large impact on steady-state $\delta^{13}C$-DIC beyond the $\delta^{13}C$ imprint of the CO_2 source alone. Whereas steady state simply requires that the $\delta^{13}C$ of outgassing CO_2 in each bottle must be equal to the $\delta^{13}C$ of the CO_2 source (-27.0‰), relating the $\delta^{13}C$ of DIC to that of the CO_2 source can not be accomplished casually without the use of equilibrium constant expressions and isotopic enrichment factors.

An analogous steady-state approach is useful in all aquatic systems where DIC turns over rapidly due to high CO_2 fluxes. For instance, in rivers of the carbonate-free Amazon lowlands (where piston velocity (K) > 2 m/d (ref. 1), typically pCO_2 > 5000 ppm and DIC < 500 μM (Table S2), and assuming river depth < 10 m) turnover time is less than 13 days and in most cases only 2-4 days, which is short relative to the large river lengths and corresponding long water residence times in the river system[29]. In small streams where pCO_2 is greater and water depths are shallower, turnover times < 1 day are likely. Other evidence for quasi-steady state is the relatively small downstream rate of change of DIC isotopes in all carbonate-free rivers except the Ji-Parana

headwaters (sites 28-31), where vegetation transitions occur. Previous studies in the highly supersaturated Amazon mainstem have also indicated the existence of a quasi-steady state between evasion and *in situ* respiration with respect to CO_2 and $^{13}CO_2$ fluxes[7,8]; $\delta^{13}C$ of CO_2 evading from the river is the same as that produced during respiration[7], while tributary DIC and ^{13}C-DIC inputs account for mainstem downstream changes[7,8]. Together the evidence suggests that dynamic equilibrium or quasi-steady state between evasion and respiration with respect to CO_2, $^{13}CO_2$, and $^{14}CO_2$ is a reasonable first-order assumption at sites not influenced by continuing dissolution of carbonate minerals, where data to construct complete mass balances are not available. The implication is that at these sites, the $\delta^{13}C$ and $\Delta^{14}C$ of evaded CO_2 gas should be equivalent to the isotopic signature of respired OC.

In systems where carbonate mineral dissolution is active or DIC turnover times are low, this steady state approach may not be valid as the river approximates a closed system. For instance, using values for the Hudson River from Cole and Caraco[2] (where K = 0.8 m/d and pCO_2 < 2000 ppm, and assuming depth = 10 m), the turnover time of DIC is > 220 days. Therefore, these systems are far from steady state and are likely still degassing the initial DIC resulting from carbonate mineral dissolution. In this case, the $\delta^{13}C$ of DIC is determined by the mass balance of the multiple sources and sinks to DIC (carbonate minerals + CO_2 from respiration – CO_2 evasion), and pH controls the $\delta^{13}C$ of CO_2 evading from the river relative to that of DIC.

CO_2 and organic carbon sources. To assess the influence of carbonate weathering on river geochemistry, we examined the inorganic solute composition at each site relative to guidelines suggested by Stallard and Edmond[15] (Fig. S1). This approach identifies as carbonate-influenced all mountain and mixed sites, and five lowland sites (Figs. 1 & S1, sites 10, 41, 42, 43 & 45). The remaining 25 lowland sites (38 samples, including those presented in Fig. 3) have little potential for direct

carbonate mineral contributions to DIC, and contain CO_2 that is predominantly contemporary (Table 1, Fig. 2).

CO_2 in carbonate-free rivers is generally isotopically distinct from the associated OC fractions (DOC, FPOC, and CPOC; Fig. 2). A $\Delta^{14}C$ comparison of CO_2 against OC fractions at the 5 carbonate-free sites where CO_2 and at least two OC fractions were measured concurrently (Table S3, 1996 samples from sites 6, 24, 28, 32 & 40) yields mixed results. CO_2 is considerably younger than DOC (the primary OC fraction) in 2 out of 3 observations, but is undistinguishable from FPOC ($\Delta^{14}C$-CO_2 = 122±15‰ vs. $\Delta^{14}C$-FPOC = 130±11‰, n=5); in these rivers, FPOC on average makes up only ¼ of total OC and is characterized by low fine suspended sediment (FSS) concentrations and high %weight (Table S2). CPOC is also older than CO_2 but makes up a very small fraction of total OC.

While the above $\Delta^{14}C$ comparison between CO_2 and OC is limited, it can be extended first with samples from the Rio Negro mouth and several small Negro streams where DIC and DOC samples were collected 7 years apart (2002 vs. 1995, sites 32 – 39). OC in these clear and blackwater rivers is strongly dominated by DOC (Table S2). Comparing $\Delta^{14}C$ offsets against sampling year atmospheric $\Delta^{14}C$-CO_2, the DOC offset (63±66‰, n=8) is 3 times the CO_2 offset (19±12‰, n=8). While the difference in the means is not statistically significant (p = 0.0850, Student's t-test for independent samples), high DOC variance is largely the result of one outlier with an even larger atmospheric offset of 217‰; excluding this value yields a DOC offset of 41±25‰ and a marginally significant difference with respect to the CO_2 offset (p = 0.0440). Second, $\Delta^{14}C$-OC in lowland samples potentially influenced by carbonates (Table S3, 1996 samples from sites 10, 41, 43 & 45) is characterised by a similar DOC atmospheric $\Delta^{14}C$ offset of 73±64‰ (n=4). The FPOC offset (-79±35‰, n=4) indicates substantial aging at these sites which, except for the Guapore (site 10), are characterised by high FSS and

low %weight FPOC values comparable to the Amazon mainstem[30] (Table S2). Therefore, while scatter is substantial, DOC – the dominant lowland OC fraction – is generally just under a decade in age; in carbonate-free lowland systems, DOC is older than CO_2. FPOC represents a more heterogeneous but less important component of total OC in such systems.

Carbonate-free lowland $\delta^{13}C$-CO_2 is generally enriched with respect to all OC fractions (Tables 1 & S3, Fig. 2). The separation for coincident samples is over 8‰, with $\delta^{13}C$-CO_2 = -20.1±3.5‰ (n=5), $\delta^{13}C$-DOC = -28.7±1.5‰ (n=3), $\delta^{13}C$-FPOC = -29.2±2.3‰ (n=5), and $\delta^{13}C$-CPOC = -28.4±0.9‰ (n=3). For Rio Negro basin DIC and DOC samples collected 7 years apart, $\delta^{13}C$-CO_2 = -25.2±0.9‰ (n=8) and $\delta^{13}C$-DOC = -29.2±0.1‰ (n=8). ^{13}C separation between CO_2 and OC is smallest in the Rio Negro basin, where C_4 grasses are rare, and largest in the Ji-Parana basin, where deforestation has led to widespread replacement of forest by C_4 pastures, even along stream corridors[24]. Lowland $\delta^{13}C$-OC observations in this study are similar to those obtained previously[7,24,30].

Influence of carbonate weathering in mountain and mixed sites. Mountain and mixed river sites contain older dissolved CO_2 ($\Delta^{14}C$ = 96 to -749‰, Fig. 2) resulting in large part from carbonate mineral dissolution involving the chemical reaction $CaCO_3(s) + H_2CO_3(aq) = Ca^{2+}(aq) + 2HCO_3^-(aq)$. Although the dissolution of carbonates increases DIC, it also increases pH, with the net result of decreasing dissolved free CO_2 concentrations and reducing evasion fluxes. Thus, while carbonate dissolution has a large impact on the isotopic signature of evaded CO_2, it can not be the main driver of outgassing. Observed CO_2 supersaturation must be maintained by a continuous flux of CO_2 from OC respiration or other CO_2 sources. These fluxes and the resulting CO_2 outgassing will gradually flush out DIC originally exported from carbonates in terrestrial settings, replacing its isotopic signature with that of the new

CO_2 source. Indeed, a CO_2 trend of increasing $\Delta^{14}C$ and decreasing $\delta^{13}C$ is observed from the Andes down to the mainstem Amazon (Fig. 2). However, this flushing is not rapid. In the mainstem of the forested middle and lower Ucayali basin, major ion geochemistry indicates that carbonate dissolution remains a dominant source of DIC from the Andean foothills to the sedimentary lowlands nearly 2000 km downstream[15] (from site 56 to site 48, Figs. 1 & S1); consequently, $\Delta^{14}C$-CO_2 remains substantially depleted (-138‰ at downstream site 48) despite likely high respiratory inputs that steadily increase CO_2 concentrations from 560 to 3150 ppm (Table S2). Over the next 2000 km downstream (from sites 47 and 48 to site 1) carbonate sediments become less prevalent and respired CO_2 gradually flushes out aged DIC, as observed in $\Delta^{14}C$-CO_2 increases from approximately -167‰ to a mean of 49‰, still below contemporary atmospheric $\Delta^{14}C$ levels. Therefore, all along the middle-lower Ucayali and western-central mainstem, inputs of young CO_2 from *in situ* respiration and tributary inflow drive large gas evasion fluxes of aged CO_2 originating from carbonate dissolution; partitioning of DIC from HCO_3^- to H_2CO_3 due to a lowering of pH (e.g., at the confluence of blackwater and whitewater rivers) may be a significant CO_2 source only near the central mainstem (Table S2).

Specific site references from the discussion. Limitations on the length of the manuscript prevented the inclusion of relevant site ID references for all discussions. This section collects such references to facilitate data interpretation. In Figure 3, Ji-Parana sites include site IDs 24, 25 & 28, while the Rio Negro mouth is site 32. The second, smaller group of observations in carbonate-free lowland sites referred to in the text includes 3 streams (sites 22, 29 & 31) and 2 mid-sized rivers (sites 6 & 7). Submerged grasses were present only in small Ji-Parana streams, at sites 22 & 23. In the central Amazon mainstem site (site 1), $\Delta^{14}C$-CO_2 reaches approximately 49‰, still below atmospheric levels. The Vilcanota river in the arid mountain headwaters of the

Ucayali, in Peru, includes three sites (sites 57, 58 & 59) highly depleted in ^{14}C that appear to be influenced by solid-earth degassing.

Supplementary Tables

Supplementary Table S1. Site and drainage area characterisation. Latitude (Lat) and Longitude (Lon) are in decimal degrees. A few sites represent aggregated data from distinct sites in relative proximity. Site numbers 17 – 31 are in the Ji-Parana basin (see Fig. 1) and their site names correspond to codes used in previous studies[24]. Continued on next page.

Site #	River	Site Name	Lat °S	Lon °W	Area km^2	Elevation		
						Site M	Basin Mean m	% > 1000 m
				Lowland				
6	Candeias	Candeias	8.766	63.708	13,200	77	179	0.2
7	Azul	Azul	9.627	64.942	4,030	103	184	0.0
9	Novo	Novo	14.172	59.742	150	295	314	0.0
10	Guaporé	Vila Bela	14.993	59.958	21,660	193	335	0.0
17	Ji-Paraná	JIP-5	8.147	62.787	73,410	69	246	0.0
18	Ji-Paraná	JIP-4	8.947	62.057	67,640	91	257	0.0
19	Machadinho	MAC	9.507	62.047	2,970	198	198	0.0
20	Ji-Paraná	JIP-3	10.092	61.977	43,580	181	284	0.0
21	Jarú	JARU	10.102	61.996	7,410	180	254	0.0
22	Boa Vista	NS1	10.757	62.368	< 10	296	297	0.0
23	Boa Vista	NS2	10.753	62.372	< 10	296	298	0.0
24	Ji-Paraná	JIP-2	10.937	61.957	29,770	192	293	0.0
25	Urupá	URUPA	10.902	61.962	4,820	191	264	0.0
26	Rolim de Moura	ROLIM	11.445	61.731	2,060	200	236	0.0
27	Ji-Paraná	JIP-1	11.452	61.463	19,170	200	325	0.0
28	Comemoração	COM-2	11.667	61.188	6,740	199	372	0.0
29	Comemoração	COM-1	12.718	60.173	160	594	598	0.0
30	Pimenta Bueno	PB-2	11.703	61.192	8,650	197	321	0.0
31	Pimenta Bueno	PB-1	12.847	60.343	130	495	491	0.0
32	Negro	Mouth	3.063	60.302	716,770	29	185	1.1
33	Barro Branco	Reserva Ducke 1	2.932	59.978	< 10	59	58	0.0
34	Cabeça Branca	Reser. Campinas 1	2.582	60.022	< 10	99	98	0.0
35	Cueiras	Cueiras	2.781	60.442	3,280	40	85	0.0
36	Asu	Reserva ZF2 1	2.608	60.216	< 10	67	67	0.0
37	Miratucu	Miratucu 4	1.963	61.848	520	34	32	0.0
38	Miratucu	Miratucu 3ag	2.031	61.853	450	34	32	0.0
39	Cobra	Miratucu 2c	2.027	61.813	< 10	34	34	0.0
40	Purus	Mouth	3.747	61.433	362,900	32	138	0.0
41	Purus	Boca do Acre	8.732	67.378	111,630	100	235	0.0
42	Acre	Brasileia	11.002	68.764	7,820	250	296	0.0
43	Juruá	Mouth	2.722	65.803	217,370	56	176	0.0
44	Japurá	Mouth	1.817	65.683	260,010	55	255	3.4
45	Juruá	Cruzeiro do Sul	7.622	72.637	43,960	188	259	0.0

Supplementary Table S1 continued. Site and drainage area characterisation.

Site #	River	Site Name	Lat °S	Lon °W	Area km^2	Elevation Site m	Elevation Basin Mean m	Elevation % > 1000 m
				Mixed				
1	Amazon	Manacapuru	3.322	60.612	2,238,490	28	560	13.4
2	Amazon	Itapeua	4.053	63.017	1,818,270	38	661	16.5
3	Amazon	Vargem Grande	3.279	67.853	1,016,030	70	1040	28.3
4	Madeira	Mouth	3.450	58.798	1,381,590	20	501	11.7
5	Mamoré	Guayaramerin	10.848	65.347	601,470	120	541	12.5
8	Madeira	Madeira at Abunã	9.677	65.417	906,120	127	681	17.8
11	Beni	Riberalta Arriba	11.022	66.128	118,330	135	1372	46.2
46	Napo	Napo	3.295	72.632	110,300	103	651	16.5
47	Marañón	Marañón	4.528	73.568	358,170	113	1106	35.6
48	Ucayali	Ucayali	4.522	73.487	341,200	112	1658	41.7
50	Pachitea	Mouth	8.733	74.572	27,500	165	830	21.1
				Mountain				
12	Beni	Rurrenabaque	14.542	67.548	68,130	504	2191	79.0
13	Alto Beni	Sapecho	15.617	67.330	29,590	608	2735	91.6
14	Achumani	Achumani	16.472	68.063	230	3834	4565	100.0
15	Yara	Yara Caranavi	15.777	67.588	340	1012	1550	84.4
16	Zongo	Zongo	16.253	68.118	260	4555	4519	100.0
49	Ucayali	Ucayali at Pachitea	8.783	74.553	205,520	165	2500	65.7
51	Tambo	Mouth	10.787	73.773	121,290	286	3199	84.6
52	Apurimac	Cunyac	13.567	72.589	22,760	2425	4105	100.0
53	Urubamba	Mouth	10.757	73.712	61,070	288	1890	51.3
54	Yanatili	Quellouno	12.602	72.533	3,020	1083	3089	98.3
55	Urubamba	Sahuayaoti	12.646	72.538	13,920	824	3791	97.1
56	Urubamba	Quillabamba	12.867	72.682	12,640	1142	4001	99.3
57	Urubamba	Pachar	13.273	72.250	9,290	3106	4284	100.0
58	Salcca	Salcca	14.102	71.422	3,190	3792	4743	100.0
59	Vilcanota	Tinta	14.166	71.402	1,610	3571	4239	100.0
60	Lago Langui-Layo	Langui	14.437	71.292	470	3877	4276	100.0

Supplementary Table S2. Average geochemical properties for isotopic sampling sites, based on samples analysed for carbon isotopes. Data used for averages are based only on samples where a ^{14}C measurement was made. Continued on next page.

Site #	Temperature °C	pH	Alkalinity μeq L^{-1}	FSS mg L^{-1}	FPOC %wt	CO_2 ppm	DIC μmol L^{-1}	DOC mg L^{-1}	FPOC mg L^{-1}	CPOC mg L^{-1}
					Lowland					
6	25.4	5.92	98	19.1	7.13	7640	362	1.65	1.36	0.13
7	25.1	5.94	77	14.7	9.91	5723	275	0.69	1.46	
9	24.7	6.41	98	15.6	9.42	2476	184	0.68	1.47	0.93
10	20.9	6.53	410	14.4	7.83	7837	681	3.41	1.13	0.19
17	31.5	7.07	344	11.6		2099	404	2.04		
18	30.1	7.13	205	7.6		1063	236	2.57		
19	29.3	6.72	125	13.7		1653	175	2.02		
20	30.1	7.39	243	17.0		692	263	4.38		
21	29.6	7.45	532	14.4		1312	570	4.75		
22	25.9	6.31	594	9.2		10300		5.98		
23	25.7	6.60	694	6.7		7100		4.36		
24	26.5	6.97	248	21.9	5.71	1525	300	2.78	0.88	0.10
25	28.3	6.97	703	47.7		3193	797	8.43		
26	29.6	7.44		26.0				2.68		
27	29.3	7.15	131	14.8		643	150	2.43		
28	25.2	6.25	39	20.7	9.60	1346	85	2.49	1.12	0.18
29	23.6	5.32	3	15.0	1.96	1872	70	1.60	0.53	
30	28.9	7.12	197	14.0		1031	229	4.02		
31	25.5	5.83	4	6.3		565	25	1.36		
32	29.0	4.87	4	6.1	13.65	5197	184	10.24	0.61	0.01
33	24.9	4.15	0			33550	1153	3.54		
34	25.5	3.94	0			26145	896	34.94		
35	30.3	3.84	0	7.7		1205	41	6.74		
36	24.8	4.02	0			7375	252	9.11		
37								7.02	0.77	
38								6.21	0.69	
39								6.09	0.39	
40	26.9	5.94	135	16.3	5.91	10048	482	4.02	0.96	0.01
41	26.4	7.68	2047	121.4	1.22	2757	2137	2.18	1.48	0.08
42	23.7	7.99	1467	70.2	2.92	964	1494	2.15	2.05	0.07
43	24.6	6.61	497	106.4	1.60	7824	767	3.50	1.70	0.05
44	25.7	5.30	15	19.9	3.64	4920	185	3.48	0.73	0.07
45	26.7	6.51	858	257.1	1.20	17173	1452	5.77	3.07	

Supplementary Table S2 continued. Average geochemical properties for isotopic sampling sites, based on samples analysed for carbon isotopes.

Site #	Temperature °C	pH	Alkalinity μeq L^{-1}	FSS mg L^{-1}	FPOC %wt	CO_2 ppm	DIC μmol L^{-1}	DOC mg L^{-1}	FPOC mg L^{-1}	CPOC mg L^{-1}
					Mixed					
1	27.7	6.37	338	161.7	1.14	8302	625	4.45	1.45	0.47
2		6.93	525	114.0	1.60	4010	663	3.98	1.79	
3		7.49	1269	203.0	1.00	2633	1358	2.68	1.95	
4	27.3	6.68	265	671.7	0.56	3551	388	2.57	3.76	0.20
5	27.3	6.67	570	421.9	0.56	8216	833	5.06	2.35	0.04
8	26.6	6.85	600	276.3	1.14	5482	789	3.59	3.15	
11	27.8	7.02	684	630.6	0.31	4431	823	1.98	1.93	0.47
46	29.7	6.94	270	178.9	1.51	2689	455	2.44	2.71	1.11
47	26.0	6.97	790	333.1	1.67	5356	957	4.66	5.58	1.49
48	28.0	7.43	1280	337.9	1.11	3149	1419	2.65	3.73	0.25
50	24.8	7.75	1290	269.2	1.84	1388	1257	2.21	4.95	7.24
					Mountain					
12	27.7	6.95	481	851.0	1.30	3658	597	1.89	8.40	0.61
13	23.9	7.76	762	1340.0	0.91	870	790	1.28	6.87	0.42
14	10.2	8.62	814	553.0	0.40	103	808	0.94	1.81	0.03
15	24.6	7.71	283			357	295	1.80	1.99	
16	6.7	7.01	203		0.73	1036	266	0.04	0.69	0.04
49	26.1	7.70	1170	288.5	1.24	1623	1315	1.80	3.58	0.73
51	25.7	7.91	1170	250.8	1.47	921	1192	2.35	3.69	0.11
52	22.1	8.75	1960	6.6	8.84	205	1833	1.57	0.59	0.00
53	27.0	8.06	960	268.5	1.67	587	1066	1.81	4.50	0.97
54	23.3	7.67	470	59.8	1.16	704	534	1.08	0.69	0.20
55	23.5	8.28	1230	46.7	2.44	446	1340	1.40	1.14	0.09
56	19.7	8.21	1390	55.0	2.73	562	1438	2.41	1.50	0.03
57	17.6	7.89	2960	183.6	3.84	2572	3183	3.40	7.04	0.01
58	15.1	7.55	2060	289.5	1.15	3872	2259	1.32	3.33	6.63
59	18.7	7.69	3320	4.5	16.16	4103	3252	2.63	0.72	0.01
60	11.9	8.46	1900	1.5	30.27	400	1821	1.90	0.45	

Supplementary Table S3. Isotopic composition (‰) of each carbon fraction in each sample. Continued on next page.

Site #	Date	DIC	CO_2		DOC		FPOC		CPOC	
		$\delta^{13}C$	$\Delta^{14}C$	$\delta^{13}C$	$\Delta^{14}C$	$\delta^{13}C$	$\Delta^{14}C$	$\delta^{13}C$	$\Delta^{14}C$	$\delta^{13}C$
					Lowland					
6	7/2/1996	-19.3	100	-20.6			136	-30.8	208	-29.3
7	6/27/1996	-19.4	85	-20.8						
9	7/5/1996	-13.2	109	-16.8						
10	7/6/1996	-21.0	-145	-25.3	271	-26.6	-18	-31.6		
17	9/20/2000	-11.8	91	-17.7						
18	9/13/2000	-10.4	106	-16.6						
19	9/13/2000	-14.5	100	-19.4						
20	9/16/2000	-10.5	93	-17.1						
21	9/16/2000	-11.9	104	-18.7						
22	8/26/2002	-13.1	59	-16.8						
22	12/2/2002	-12.9	102	-14.3						
22	1/15/2003	-9.5	98	-13.9						
23	8/28/2002	-10.9	111	-16.4						
23	12/5/2002	-9.5	104	-13.2						
24	7/3/1996	-10.0	118	-15.6	245	-27.0	125	-25.6	12	-27.6
24	9/17/2000	-10.5	106	-17.3						
24	1/26/2003	-16.3	86	-20.3						
25	9/12/2000	-11.5	111	-17.8						
25	1/24/2003	-11.2	98	-16.5						
26	9/11/2000	-11.6	102	-18.4						
27	9/11/2000	-12.0	96	-18.3						
28	7/3/1996	-14.9	128	-17.7			139	-28.6	143	-28.1
28	9/11/2000	-16.0	100	-19.5						
28	1/18/2003	-20.4	88	-22.6						
29	7/4/1996	-20.5	62	-19.8						
29	9/10/2000	-21.8	74	-21.8						
30	9/11/2000	-12.9	94	-19.2						
31	9/10/2000	-19.0	28	-20.0						
32	1/31/1995				181	-29.1				
32	6/20/1995				336	-29.1	121	-29.1		
32	7/6/1996	-25.4	141	-24.4	130	-29.3	138	-29.8		
32	7/15/2002	-27.2	118	-26.2						
32	11/12/2002	-24.2	99	-24.1						
33	7/13/1995				151	-29.3				
33	7/13/2002	-25.0	115	-23.9						
34	12/12/1995				107	-29.1				
34	7/13/2002	-27.5	84	-26.3						
34	11/3/2002	-26.5	102	-25.4						
35	7/15/2002	-26.3	90	-25.2						
36	7/19/2002	-25.9	89	-24.7						
36	11/6/2002	-26.8	95	-25.7						
37	3/30/1995				169	-29.1				
38	3/29/1995				175	-29.2				
38	4/2/1995				171	-29.4				
39	4/2/1995				167	-29.4				
40	7/5/1996	-21.0	124	-22.4	96	-29.9	113	-31.5		

Supplementary Table S3 continued. Isotopic composition (‰) of each carbon fraction in each sample.

Site #	Date	DIC	CO_2		DOC		FPOC		CPOC	
		$\delta^{13}C$	$\Delta^{14}C$	$\delta^{13}C$	$\Delta^{14}C$	$\delta^{13}C$	$\Delta^{14}C$	$\delta^{13}C$	$\Delta^{14}C$	$\delta^{13}C$
					Lowland					
41	6/23/1996	-13.8	72	-21.1	175	-29.3	29	-30.8		
42	6/22/1996	-14.6	2	-22.1						
43	7/1/1996	-17.9	113	-22.5	116	-29.9	59	-30.0		
44	7/2/1996	-17.6	110	-17.1						
45	6/25/1996	-15.4	68	-19.5	172	-29.7	55	-29.8	85	-28.7
					Mixed					
1	1/10/1995				201	-29.4	-85	-28.3	-183	-28.7
1	6/16/1995				138	-29.6	-157	-28.7	-127	-27.8
1	7/6/1996	-17.7	76	-21.4						
1	7/12/2002	-18.3	30	-20.5						
1	7/12/2002	-18.7	42	-20.4						
2	8/26/1991	-12.7	36	-18.6						
3	8/12/1991	-11.4	-29	-18.5						
4	1/19/1995				331	-28.7	-73	-27.4	-148	-27.4
4	7/8/1996	-15.8	96	-20.7	155	-28.8	-49	-29.8		
5	5/3/1995						-329	-27.3	-93	-26.1
8	6/27/1996	-13.8	49	-19.4	197	-28.0	-131	-28.3	-233	-26.5
11	5/6/1995				199	-28.6	-440	-26.8	-146	-27.6
46	11/7/1996	-13.7	22	-19.4	231	-29.6	-24	-28.9	-18	-28.4
47	11/8/1996	-11.6	-196	-17.7	157	-29.2	-6	-28.5	-43	-28.1
48	11/8/1996	-11.5	-138	-18.4	158	-29.5	-59	-28.6	-124	-28.2
50	11/5/1996	-11.1	-142	-18.7						
					Mountain					
12	11/14/1994	-9.9	-154	-15.8						
13	11/15/1994	-6.9	-116	-14.2						
13	5/11/1995								-30	-27.5
14	11/20/1994	-5.4	-61	-14.9						
15	11/16/1994	-6.9	15	-14.5						
16	5/15/1995						-221	-25.6	51	-27.6
49	11/5/1996				271	-28.7	-80	-28.1	35	-28.6
51	11/1/1996	-6.1	-155	-13.7	153	-27.9	-73	-27.6	80	-28.3
52	10/21/1996	-2.6	-148	-10.8	27	-21.8	19	-23.7	-19	-23.8
53	11/1/1996	-10.0	-151	-17.5	111	-29.0	-301	-27.1	75	-28.5
54	10/27/1996	-3.5	-45	-11.1						
55	10/27/1996	-3.3	-248	-11.3						
56	10/27/1996	-3.3	-273	-11.7	221	-25.2	-89	-24.3	17	-26.2
57	10/26/1996	-3.0	-645	-11.5						
58	10/23/1996	-2.4	-749	-10.7			-613	-24.6	-208	-25.9
59	10/23/1996	-2.8	-523	-10.9	-222	-23.3	-257	-24.6	-353	-26.4
60	10/24/1996	-2.0	-109	-11.3						

Supplementary Figure

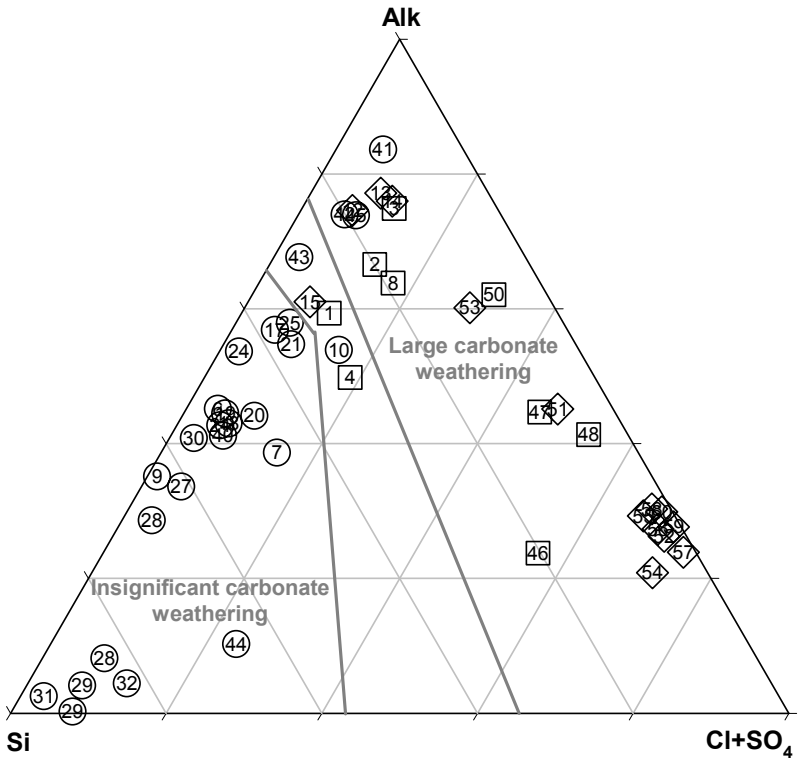

Supplementary Figure S1. Relative proportions of silica (μmol L^{-1}), alkalinity (μeq L^{-1}), and $Cl^- + SO_4^{2-}$ (μeq L^{-1}), indicative of dominant weathering regimes controlling the dissolved load[15]. Legend is as in Fig. 1. Only samples with ^{14}C-DIC analyses are shown. Data were not corrected for seasalt aerosols. Rivers falling near the alkalinity and $Cl^- + SO_4^{2-}$ vertices are cation-rich and drain areas rich in carbonate sediments and evaporites + carbonates, respectively, whereas rivers draining cation-poor aluminosilicates cluster near the silica vertex[15]. We delineated regions of high vs. insignificant carbonate weathering contributions[15]. A heterogeneous set of five intermediate sites was assigned to the carbonate influence group. Seven additional lowland sites where silica,

alkalinity, and major anions were not measured were assumed to be carbonate-free based on dominant lithology, observations from neighbouring rivers, or previous studies. All mountain and mixed sites, and five lowland sites (sites 10, 41, 42, 43 & 45), are identified as carbonate-influenced.